TRAPICHE TOURMALINE FROM ZAMBIA

Thomas Hainschwang, Franck Notari, and Björn Anckar

Well-formed crystals of green tourmaline from northwestern Zambia show a growth pattern reminiscent of trapiche emerald/ruby when sliced perpendicular to the c-axis. In fact, such slices were originally encountered in parcels sold as emerald in Zambia. The trapiche appearance most likely originates from skeletal growth, with the pattern formed by a black carbonaceous substance (mostly graphite) that partially filled growth tubes concentrated in three areas: (1) along the three edges of the trigonal pyramids *r* {$10\bar{1}1$} or *r'* {$01\bar{1}\bar{1}$}, (2) at the interface between the trigonal pyramids and the prism *a* {$11\bar{2}0$}, and (3) between individual growth sectors of the prism *a*. Spectroscopic and chemical analyses indicate that the tourmaline is uvite that is colored green by a vanadium-related mechanism. To the authors' knowledge, this is the first occurrence of trapiche tourmaline.

Tourmaline is one of the most complex minerals in terms of its chemical composition and color distribution. The extraordinary color zoning of many tourmalines was illustrated by Benesch (1990). Triangular zones containing a trigonal star-like pattern (following the edges of the trigonal pyramid) are common in some multicolored tourmalines, particularly in liddicoatite from Madagascar. Other growth phenomena are not common in tourmaline, so two of the authors (TH and FN) were interested when, in November 2005, they encountered some sliced crystals of green tourmaline from Africa that exhibited a growth structure similar to the trapiche pattern known to occur in emerald and ruby (see, e.g., figure 1). The third author (BA) first saw such material in 2004 and 2005 in Lusaka, Zambia, within "salted" parcels of rough emerald and as separate lots of this green tourmaline that were being offered as emerald (figure 2). Zambian gem traders called the material "Mercedes Benz tourmaline" (or "emerald") due to the shape of the trapiche-like inclusions in the cores of the slices, which may resemble this automobile company's logo (again, see figure 1).

LOCATION AND PRODUCTION

Most of this trapiche tourmaline reportedly comes from the Kavungu mine adjacent to the tiny village of Jivunda in Chief Sailunga's area, which lies southeast of Mwinilunga in northwestern Zambia (figure 3). The locality is accessed by driving 230 km west from Solwezi on the Mwinilunga road and turning south for 35 km to reach Jivunda on the road going toward Ntambu. Local gem traders also report another locality for this tourmaline in the Kampanda area, which is located southwest of Mwinilunga near the border with Angola.

According to the Jivunda villagers, the Kavungu deposit has been known for at least 10 years, but it was not significantly exploited until 2004, when commercial mining was attempted under the assumption the material was emerald. However, this activity was short-lived, and the equipment was removed when the mine investor realized that the gems were another mineral altogether. Children

See end of article for About the Authors and Acknowledgments.
GEMS & GEMOLOGY, Vol. 43, No. 1, pp. 36–46.

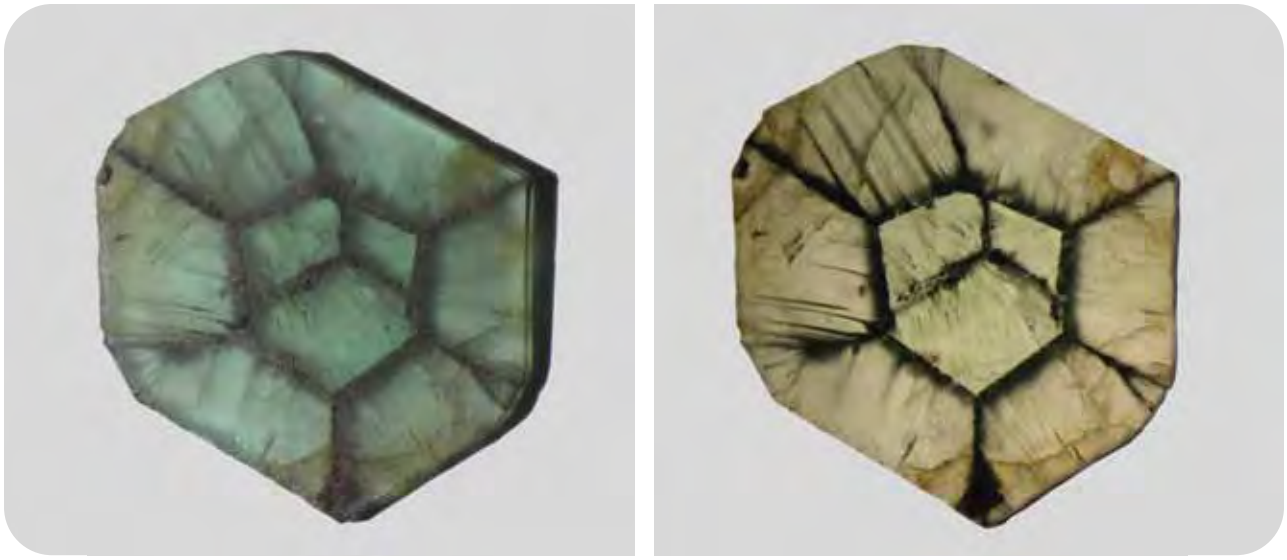

Figure 1. A distinct trapiche pattern is seen in this tourmaline slice (12.8 × 10.6 mm) from Zambia. Photos by T. Hainschwang (left—overhead light; right—transmitted light).

from Jivunda continue to recover the tourmaline by hand from the various pits dug over the years (see, e.g., figure 4), which they sell to passing traders. The tourmaline is fairly abundant; during a two-hour mine visit in December 2006, one of the authors (BA) witnessed the recovery of more than 100 crystals by a few of the children. It must be noted, though, that only about 1–2% of the tourmaline is found as near-euhedral to euhedral crystals that are suitable for slicing or cutting thin cabochons that show the trapiche pattern. Facetable material is extremely rare and restricted to small pieces (<0.10 ct), due to the dark color of the tourmaline. For these reasons, the trapiche tourmaline is seldom encountered on the international market.

GEOLOGY

The bedrock at the Kavungu mine consists of an impure and distinctly banded marble that has been selectively weathered into a typical karst landform, with solution-resistant areas of marble that are surrounded by lateritic soil (figures 4 and 5). The tourmaline has been found only in these residual laterite

Figure 2. Well-formed crystals of green tourmaline—which may display a trapiche appearance when cut into slices—have been sold as emerald in Zambia. The crystals shown here range from 0.8 to 2.6 cm long. In general, only a small percentage of the tourmaline shows a near-euhedral shape and a noticeable trapiche pattern when sliced. Gift of Björn Anckar, GIA Collection no. 36754; photo by Robert Weldon.

Figure 3. The trapiche tourmaline studied in this report came from the Kavungu mine, located southeast of Mwinilunga in northwestern Zambia. Similar tourmaline has also reportedly been found in the Kampanda area, which lies southwest of Mwinilunga near the Angolan border.

Figure 4. Previous mining efforts have left several pits at the Kavungu site. Tourmaline is encountered in the lateritic soil between the marble outcrops. Photo by B. Anckar, December 2006.

layers, so its precise petrologic setting is unknown. Villagers report that the tourmaline crystals are occasionally seen "in the hard rock," but no such sample was encountered at the time of the visit by author BA.

The Kavungu mine area is underlain by metasedimentary rocks of the Wamikumbi Formation of the Neoproterozoic Katanga System (Klinck, 1977). The Katanga System has been affected by three deformation phases of the Lufilian orogeny. The immediate area of the Kavungu mine was initially mapped as biotite schists (see map appended to Klinck, 1977). More recently, the Geological Survey Department remapped the Kavungu mine area as dolomitic marbles (D. Lombe and E. Mulenga, pers. comm., 2006). Klinck (1977) studied the area but did not encounter the tourmaline locality. He did, however, describe a location only 2 km southeast of the Kavungu mine with outcrops of banded calcite and calcite-scapolite marbles that he called the "Mujimbeji Marble Member." Both of these marbles contain abundant phlogopite, minor quartz, and accessory pyrite. Klinck (1977) also

reported that they contain minor bands of dolomitic marble and very fine-grained graphitic schist.

It is reasonable to believe that the tourmaline (which was identified as uvite; see below) is metamorphic in origin and formed within these impure Mg-bearing marbles (see, e.g., Gübelin, 1939; Anovitz and Grew, 1996), where it was most likely hosted by local graphite-bearing zones (as shown by the presence of graphite in the trapiche inclusions). Boron, which is an essential element for tourmaline crystallization, is highly mobile in metamorphic aqueous fluids. Klinck (1977) speculated that the abundance of scapolite in the marble is due to evaporite layers in the original sediments; evaporites are commonly enriched in boron.

MATERIALS AND METHODS

For this study, we examined two doubly terminated crystals (5.01 and 12.74 ct) and 30 slices of trapiche tourmaline (0.33–5.29 ct), 28 of which were cut from three similar crystals. The slices were 1–1.5 mm thick and cut perpendicular to the c-axis. In addition, 16 trapiche emeralds (14 cabochons and two crystals) from Muzo, Colombia, were examined microscopically to provide a comparison of their growth patterns and structures.

The trapiche tourmaline samples were tested by standard gemological methods for refractive index (on two polished slices) and specific gravity (determined hydrostatically for the two crystals). The fluorescence of all samples was observed using a standard long- and short-wave UV lamp (365 and 254 nm, respectively). Microscopic examination of all samples was performed in both reflected and transmitted light with a Leica MZ12 binocular microscope.

The trace-element composition of three samples (one crystal and two slices from two different crystals) was measured qualitatively with a Thermo Noran QuanX energy-dispersive X-ray fluorescence (EDXRF) system, using a Si detector cooled by a Peltier cooling stage. Quantitative chemical analysis of two other slices (26 spots total) by electron microprobe was obtained with an ARL-SEMQ instrument (15 kV accelerating voltage, 15 nA beam current, and 3 µm beam diameter). Analyses were calibrated with natural mineral and synthetic compound standards; ZAF and MAN correction procedures were applied to the data (see, e.g., Donovan and Tingle, 1996).

Polarized specular reflectance infrared spectra were recorded for three samples (one from each of the three crystals that were sliced) at 4 cm^{-1} resolution with a Perkin Elmer Spectrum BXII FTIR (Fourier-transform infrared) spectrometer equipped with a DTGS (deuterium triglyceride sulfate) detector and a fixed-angle specular reflectance accessory. We used reflectance mode, because these spectra give more precise information about the structure of the samples—specifically, detection of the intrinsic one-phonon absorptions of tourmaline—than do spectra in transmission mode.

Figure 5. Local miner and gem dealer Stanley Kabwita is shown next to an outcrop of distinctly banded marble in a pit at the Kavungu tourmaline mine. Photo by B. Anckar, December 2006.

Visible–near infrared (Vis-NIR) absorption spectra in the 400–1000 nm range were recorded for two slices (both of which had been analyzed by EDXRF and FTIR spectroscopy) on a custom-made system equipped with an Ocean Optics SD2000 dual-channel spectrometer that had a resolution of 1.5 nm. A 2048-element linear silicon charge-coupled device (CCD) detector was also used. We employed a Hitachi U-3000 spectrophotometer to collect polarized spectra of the same two slices in the UV-Vis-NIR range from 250 to 800 nm. Only the ordinary ray was determined, owing to the dark color of the tourmaline.

Micro-Raman spectra of the inclusions in one slice were recorded with a Renishaw 1000 Raman microscope using a 514 nm laser. Integration times of 10 seconds and up to three scans per spectrum were used.

For X-ray diffraction analysis, a crystal fragment of the tourmaline was mounted on a Nonius Kappa CCD diffractometer equipped with graphite-monochromated Mo-Kα radiation.

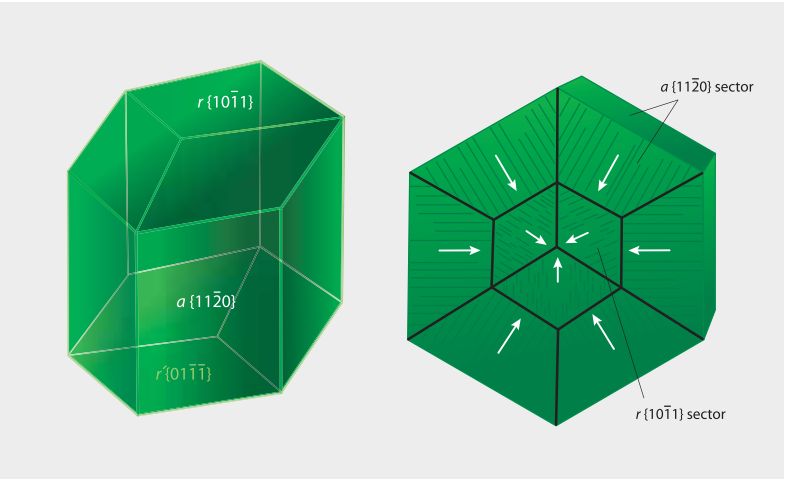

Figure 6. The trapiche tourmaline crystals consisted of the hexagonal prism a {11$\bar{2}$0} and the trigonal pyramids r *{10$\bar{1}$1} and* r′ *{01$\bar{1}\bar{1}$}; the 180° rotation of the pyramids is evident (left). An idealized drawing of a slice cut perpendicular to the c-axis is shown on the right. The arrows indicate the orientation of the channels; in the inner sectors, they are nearly parallel to the c-axis, while those in the outer sectors are close to perpendicular to the c-axis.*

RESULTS

Crystal Morphology and Trapiche Pattern. The tourmaline crystals showed an unusually well-formed and simple habit consisting of the hexagonal prism *a* {11$\bar{2}$0} that was terminated by the positive (on one end) and negative (on the other end) trigonal pyramids *r* {10$\bar{1}$1} and *r′* {01$\bar{1}\bar{1}$} (figure 6, left). As the indices of the pyramids indicate, the pyramids were rotated 180° to one another; thus, the term *polar* or *hemimorph* for tourmaline crystals in general. The prism faces were smooth, as is typical of uvite but uncommon for most other tourmalines, which have striated and rounded faces (Benesch, 1990). The basal pinacoid *c* {0001} was well developed in some crystals seen by one of the authors (BA).

The trapiche motif was formed by black inclusions that were concentrated along the three edges of the trigonal pyramid (forming the central trigonal "star"), at the interface between the trigonal pyramid and the hexagonal prism (hexagon surrounding the trigonal star), and extending from the six edges of the internal prism toward the six edges of the external prism (six outer "arms"; figure 6, right). The black inclusion material appeared to be hosted by growth channels that showed two crystallographic orientations. One set followed the vertical growth direction of the pyramidal faces (parallel to the "faces" of the core formed by the *r* sectors) making up the central trigonal star. The other set appeared at first glance to be perpendicular to the prism, but was likely inclined at the same angle as the pyramidal faces; these channels formed the six "arms" connecting the *r* sectors with the prism, and accentuated the hexagon surrounding the trigonal star. The progression of slices from each crystal showed that the pyramidal faces were dominant at one end and decreased in importance toward the other end, where growth of the prism strongly dominated (see, e.g., figure 7). This structural arrangement was present in all samples, including the two unsliced crystals. The trapiche

Figure 7. These series of slices were cut perpendicular to the c-axes of two crystals of trapiche tourmaline. Each series shows a progression in the dominance of various growth sectors, as marked by the black inclusions that form the trapiche patterns. Photos by T. Hainschwang (upper row—FN 7665–7674, up to 13.4 × 10.6 mm; lower row—TH 682–6810, ~8.4 mm in diameter).

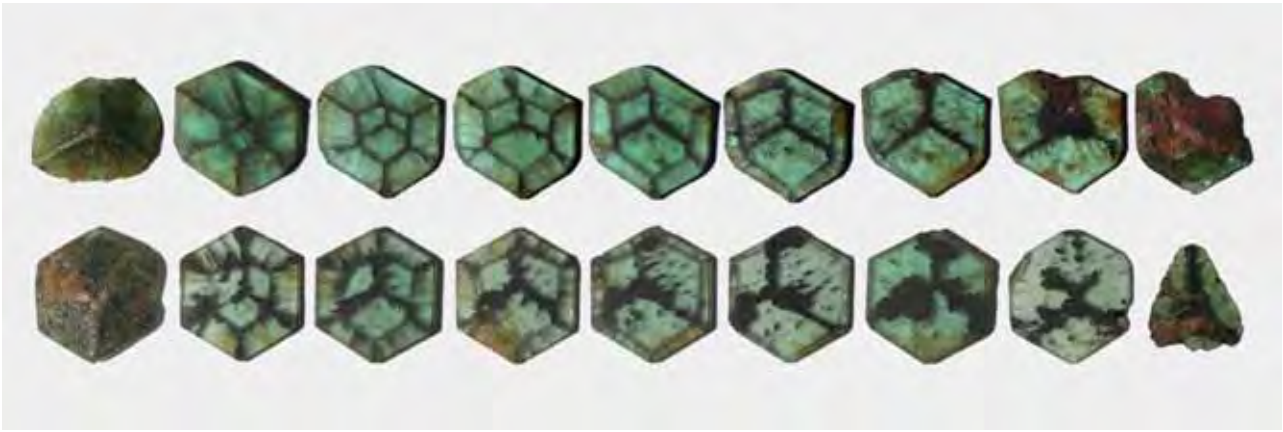

Figure 8. Chalky yellow short-wave UV fluorescence was shown by the slices and crystals of trapiche tourmaline. However, the faces of the trigonal pyramid were inert. Photos by T. Hainschwang (samples TH 682–6810; ~8.4 mm in diameter).

pattern was clearly visible only in the relatively thin slices, since the very dark green color impeded observation of the gray-to-black trapiche pattern in the uncut crystals unless they were examined with very strong transmitted light.

Standard Gemological Testing. The trapiche tourmaline had a deep green bodycolor with very weak pleochroism. The refractive indices were 1.620–1.640, yielding a birefringence of 0.020. The specific gravity varied from 2.82 to 2.99. The samples were inert to long-wave UV radiation, but they fluoresced a weak-to-moderate chalky yellow to short-wave UV on the prism faces only. However, the pyramidal faces did not show UV fluorescence (figure 8). Microscopic observation revealed that the black inclusion material responsible for the trapiche pattern was concentrated in elongate growth channels within the tourmaline (figure 9).

Chemical Analysis. EDXRF spectroscopy of the three samples identified them as Mg-Ca tourmaline with minor Na in two cases. Electron-microprobe analyses (table 1) of two other slices gave chemical compositions that correspond to near end-member uvite (Dunn, 1977a). All of the analyses performed on both slices showed nearly identical compositions, regardless of spot location (e.g., whether on the dark trapiche pattern or the green central area). Traces of the chromophores vanadium, chromium (with V>Cr), titanium, iron, and sometimes Mn also were detected in these two samples. In addition, traces of strontium were detected by EDXRF spectroscopy, and minor fluorine and traces of sodium and zinc were measured by electron microprobe; the latter technique also found minute amounts of potassium and bismuth in the dark trapiche pattern areas.

FTIR Spectroscopy. The polarized specular reflectance FTIR spectra of the trapiche tourmaline samples were almost identical to the reference spectra of most of the "chrome" tourmalines (uvite to intermediate uvite-dravite) from Landanai, Tanzania, in the authors' database. The polarized spectra showed strongly pleochroic absorptions, with the ordinary and extraordinary rays being distinctly different (figure 10). Besides the widely varying intrinsic bands between 1500 and 450 cm^{-1}, the peak at 3550 cm^{-1} (related to structural hydroxyl groups; Rosenberg and Foit, 1979) was only detected in the extraordinary-ray spectrum.

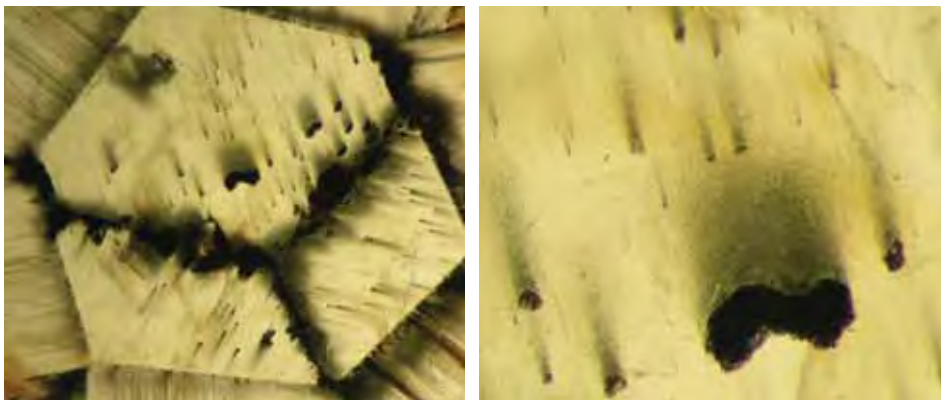

Figure 9. As seen here in transmitted light, two sets of growth channels are apparent in the trapiche tourmaline (left), one following the vertical growth direction of the pyramidal faces, and one nearly perpendicular to the prism. Some channels are empty, while others are filled with a black carbonaceous material (right). Photomicrographs by T. Hainschwang; magnified 10× (left) and 40× (right).

TABLE 1. Representative chemical composition by electron microprobe of two trapiche tourmaline slices.[a]

Chemical composition	Slice 1		Slice 2	
	Green central region[b]	Black trapiche ray	Green central region	Black trapiche ray
Oxide (wt.%)				
SiO_2	36.03	35.96	36.06	36.10
TiO_2	0.33	0.19	0.15	0.12
B_2O_3 (calc)	10.55	10.51	10.57	10.56
Al_2O_3	26.73	26.74	26.70	26.70
Cr_2O_3	0.15	0.13	0.06	0.06
Bi_2O_3	nd	nd	nd	0.08
V_2O_3	0.34	0.28	0.35	0.32
FeO	0.01	nd	0.01	nd
MnO	0.01	nd	nd	nd
MgO	15.12	14.99	15.10	15.09
CaO	5.03	4.96	5.39	5.28
ZnO	nd	nd	0.03	0.07
Na_2O	0.43	0.43	0.62	0.60
K_2O	nd	0.08	nd	0.02
H_2O (calc)	3.11	3.09	3.13	3.21
F	1.12	1.13	1.09	0.91
Subtotal	98.96	98.49	99.26	99.12
-O=F	0.47	0.48	0.46	0.38
Total	98.49	98.01	98.80	98.74
Ions on the basis of 31 (O,OH,F)				
Si	5.934	5.949	5.931	5.942
Ti	0.041	0.024	0.018	0.014
B	3.000	3.000	3.000	3.000
Al	5.190	5.214	5.177	5.180
Cr^{3+}	0.020	0.017	0.007	0.007
Bi^{3+}	nd	nd	nd	0.003
V^{3+}	0.044	0.038	0.047	0.042
Fe^{2+}	0.001	nd	0.001	nd
Mn	0.001	nd	nd	nd
Mg	3.712	3.695	3.701	3.701
Ca	0.887	0.878	0.949	0.931
Zn	nd	nd	0.003	0.008
Na	0.138	0.137	0.199	0.191
K	nd	0.018	nd	0.003
F	0.584	0.593	0.565	0.475
OH	3.416	3.407	3.435	3.526

[a]*Contents of B_2O_3 and H_2O were calculated by stoichiometry. Abbreviation: nd=not detected. Detection limits (wt.%): FeO=0.005, MgO=0.014, MnO=0.005, K_2O=0.015, ZnO=0.029, and Bi_2O_3=0.020. In addition, Cu was analyzed but below the detection limit (0.009 wt.% Cu_2O).*

[b]*The chemical composition recorded in this analysis corresponds to the following formula: $(Ca_{0.887}Na_{0.138})_{1.025}(Mg_{2.712}Al_{0.188}Ti_{0.041}Fe_{0.001}Mn_{0.001})_{2.943}(Al_{4.936}Mg_{1.00}V^{3+}{}_{0.044}Cr^{3+}{}_{0.020})_6(BO_3)_3(Si_{5.934}Al_{0.066})_6O_{18}(OH_{3.416}F_{0.584})_4$. End-member uvite has the general formula $CaMg_3(Al_5Mg)(BO_3)_3(Si_6O_{18})(OH)_4$.*

UV-Vis-NIR Spectroscopy. The ordinary-ray spectrum of the tourmaline was characterized by two broad bands, one centered at 415 nm and the other at 610 nm (figure 11). The resulting strong broad transmission window centered at 520 nm is responsible for the green coloration.

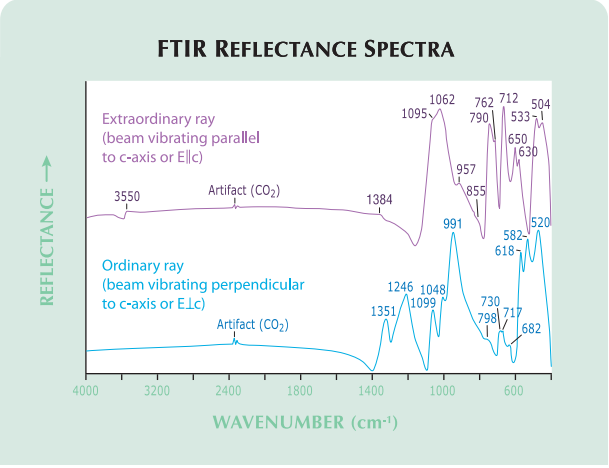

Figure 10. These polarized specular reflectance FTIR spectra are indicative of uvite. The spectral bands are very pleochroic, as shown by the variations in the absorption characteristics of the ordinary and extraordinary rays. The x-axis scale is compressed in the 4000–2000 cm^{-1} region.

Micro-Raman Spectroscopy. The Raman spectra of the black inclusions in the trapiche pattern were characterized by graphite peaks mixed with multiple unknown peaks. Raman analysis also revealed rare iron oxide inclusions—most likely hematite—and inclusions of dolomite within the trapiche pattern.

X-Ray Diffraction. X-ray diffraction analysis gave lattice parameters of a = 15.96(1) Å and c = 7.20(1) Å. The relatively high value of the lattice parameter c

Figure 11. The polarized UV-Vis-NIR spectrum of a trapiche tourmaline (ordinary ray) shows two broad bands centered at approximately 415 and 610 nm, which are characteristic for vanadium-colored green gems such as tsavorite and some tourmaline.

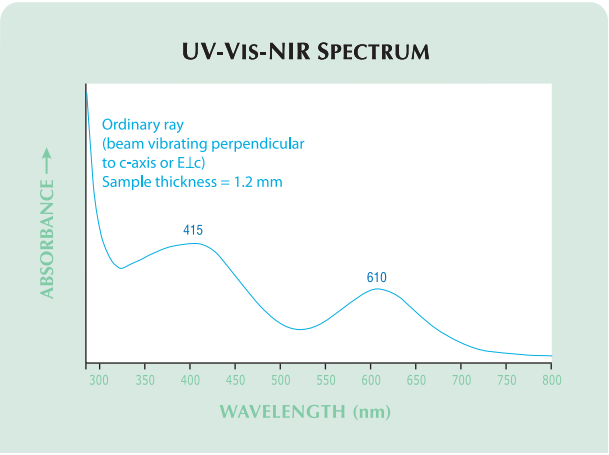

clearly indicated that there was some Mg at the Z site (~1 atom per formula unit). These parameters are consistent with the uvite species of tourmaline.

DISCUSSION

Win (2005) documented a sample of green tourmaline from Mong Hsu, Myanmar, that appeared to show a trapiche pattern. However, the authors of the present article believe that the star-like motif in that sample is due to color zoning rather than the skeletal growth that is associated with trapiche material.

The chemical and spectroscopic properties of the Zambian trapiche tourmaline identify it as near end-member uvite, with traces of Na, Fe, V, and Cr. Chemically, uvite is distinguished from other tourmalines by its Ca-Mg content, and the dravite component is indicated by Na. The identification as uvite was verified by X-ray diffraction analysis and lattice parameter calculations.

Standard gemological, spectral, and chemical data for the trapiche tourmalines correspond to those recorded for the majority of "chrome" tourmalines from Landanai, Tanzania, from the authors' database; these are, in most cases, colored by vanadium, with a minor influence from chromium (Schmetzer and Bank, 1979). The deep green color of the trapiche tourmaline also is most likely due to vanadium (V^{3+}). Although chromium and vanadium both cause broad absorption bands centered at about the same position in the UV-Vis-NIR spectrum (e.g., 600–610 [V^{3+}] and 588 nm [Cr^{3+}]; 418–440 nm [V^{3+}] and 417 nm [Cr^{3+}]; Schmetzer, 1978), the characteristic weak Cr^{3+} absorption at 687 nm (Schmetzer, 1978) was not apparent. And while the presence of Fe and Ti was confirmed by chemical analysis, the 438–444 nm band due to $Fe^{2+} \rightarrow Ti^{4+}$ charge transfer (Schmetzer, 1978) was not evident in the absorption spectra of the chemically analyzed samples. Additionally, the ratio of V:Cr determined by the chemical analyses showed that vanadium is strongly dominant. This is consistent with the UV-Vis-NIR spectra, which were uniquely characterized by the two broad bands due to V^{3+} (see also Schmetzer and Bank, 1979; Schmetzer, 1978).

Dietrich (1985) described the yellow UV fluorescence in some tourmaline (particularly uvite) as "mustard-yellow"; a similar hue was apparent in our samples (again, see figure 8). The lack of this chalky yellow luminescence on the pyramidal faces can most probably be explained by a higher iron content in those sectors at the end of crystal growth; iron impurities are known to quench yellow fluorescence in dravite and uvite (and in many other gems; Dunn, 1977a,b).

Figure 12. The trapiche pattern in the tourmaline is particularly evident when slices of the material are observed with strong transmitted light. Photo by Robert Weldon.

The trapiche pattern most likely formed by skeletal growth, resulting in microscopic channels with two crystallographic orientations: one following the vertical growth direction of the pyramidal faces (parallel to the "faces" of the core formed by the $\{10\bar{1}1\}$ sector); and one nearly perpendicular to the prism, most likely inclined at the same angle as the pyramidal faces (again, see figure 9). These channels are responsible for the significant variations in specific gravity; the greater their abundance, the lower the measured S.G. value.

The trapiche pattern is emphasized by the presence of a black carbonaceous material within these channels (figure 12). These inclusions are most likely related to the lithology of the host rock, as in trapiche emeralds from Colombia. This is supported by the presence of layers and bands of very fine-grained graphitic schist in the marble at the mine site. Our visual and microscopic observations suggest a formation process very similar to that of trapiche emeralds from Muzo, Colombia (see also box A). Muzo trapiche emerald formed in beds of carbonaceous limestone intercalated with black shale (Pogue, 1917). Another trapiche gem related to carbonates is corundum (ruby and violet-to-purple sapphire) from Myanmar, which formed in marbles via contact metasomatism (Sunagawa, 2005). The trapiche tourmaline described here most likely formed in impure Mg-bearing marbles. The close association of all three trapiche gem varieties with limestone or marble suggests that they share a similar formation mechanism.

BOX A: THE TRAPICHE GROWTH PHENOMENON

The trapiche growth phenomenon in gems is commonly associated with emeralds showing a black "fixed star"–like pattern that originate from the Muzo, La Peña, and Coscuez mines in Colombia (e.g., figure A-1). The earliest observation of such emeralds was made by Bertrand (1879). Subsequent work led to much confusion and error, such as ascribing their unusual pattern to twinning (Muñoz, 1948). The first thorough analysis of this material, with the logical conclusions pointing toward a growth phenomenon due to different growth rates, was published by Nassau and Jackson (1970).

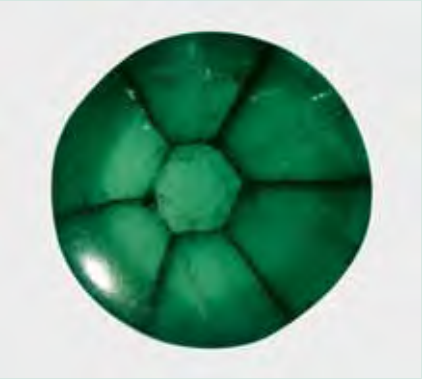

Figure A-1. These trapiche emeralds are representative of such material from Colombia. The observed pattern and the presence and orientation of growth channels are similar to the ones seen in the trapiche tourmalines. Photos by T. Hainschwang (left—TH A15, 10.8 × 8.4 mm; right—FN 6776, 8.6 × 8.4 mm).

Figure A-2. In these trapiche rubies from Mong Hsu, skeletal growth is responsible for the "star." On the left (5.7 × 5.0 mm), typical skeletal growth formed a simple star; on the right (8.2 × 6.6 mm), very strongly developed skeletal growth resulted in a star motif of the gemmy sectors that is created by triangular opaque skeletal arms. Photos by T. Hainschwang.

Figure A-3. Much of the material currently sold as "trapiche" sapphire is in fact not the result of skeletal growth. Only the star in the unusual sample on the right is due to skeletal growth; in the sample on the left, the star-shaped pattern is due to the variable exsolution of inclusions. Photos by T. Hainschwang (left—TH A18, 9.2 × 9.1 mm; right—TH A17, 6.5 × 5.7 mm).

Sunagawa (2005) attributed the trapiche phenomenon in both beryl and corundum to skeletal (or dendritic) growth, in which the edges and corners grow much faster than the faces of a crystal. This phenomenon typically occurs on rough interfaces, under conditions of rapid growth due to local buildup of undissipated latent heat on crystal faces, or simply due to undersaturation of the surrounding solution of a fast-growing crystal. In extreme cases, it can cause fine, tree-like protuberances and branching growth forms (see, e.g., Libbrecht and Rasmussen, 2003).

Trapiche rubies from Mong Hsu (Myanmar) and Vietnam were described by Schmetzer et al. (1996; see also figure A-2). An explanation for their formation was given by Sunagawa et al. (1999), who proposed dendritic (skeletal) growth followed by layer-by-layer growth. Subsequent publications cited basically the same explanation—rapid growth and changes in growth conditions—to explain the trapiche pattern in these rubies. The interpretations differed slightly from author to author (see, e.g., Garnier et al., 2002; Sunagawa, 2005), especially concerning the different growth stages and whether the skeletal arms were formed before, or at the same time as, "regular" growth.

Similar-appearing "trapiche" sapphires are also present on the market. However, these sapphires owe their "star" to variable exsolution of mineral inclusions within the different sectors (figure A-3, left; see also Schmetzer et al., 1996). In some unusual "trapiche" sapphires from Mogok, the pattern results from the distribution of chromophores, resulting in a white star-shaped pattern on a blue background (sample in author TH's collection). True trapiche sapphires resulting from skeletal growth are very rare, and the only samples the authors know of are violet-to-purple sapphires from Mong Hsu (figure A-3, right).

It is not yet clear whether there should be different nomenclatures for the various "fixed star" patterns that are being offered as "trapiche" in the marketplace, especially for sapphire. It *is* evident that true trapiche corundum (i.e., formed by skeletal growth) is much rarer than the others described above; this is particularly true for the violet-to-purple trapiche sapphires.

The trapiche phenomenon is also known in other minerals, such as quartz and andalusite, which the authors are currently studying.

Our comparison of the tourmalines to trapiche emeralds showed nearly identical growth patterns, with tubes filled by carbonaceous inclusions oriented in two crystallographic directions in both gems. The same is true for the development of the pinacoid in emerald versus the development of the trigonal pyramidal faces in tourmaline: In both, from the beginning to the end of growth, a cone-like sector developed as the result of a decrease in the pinacoid/pyramid in the positive c-axis direction and their enlargement in the negative direction. This is most evident when a crystal is sliced parallel to the prism faces (Nassau and Jackson, 1970). In the trapiche tourmaline studied here, the pyramid sector could be reconstructed by observation of the slices cut perpendicular to the c-axis (figure 7). It has been determined that in doubly terminated uvite crystals the positive direction grows about twice as fast as the negative one (Takahashi and Sunagawa, 1998). Since fast-growing faces diminish in crystals (and eventually disappear; Sunagawa, 2005), we concluded that the direction with the diminishing $\{10\bar{1}1\}$ sector core was the positive c-axis direction, and the direction with the growing $\{10\bar{1}1\}$ sector core was the negative c-axis direction.

A distinctive feature of the trapiche pattern in this tourmaline is the presence of a trigonal "star" within the core formed by the $\{10\bar{1}1\}$ sector, corresponding to the edges of the trigonal pyramid. Such a pattern is not known in either corundum or beryl; when a central sector is present in those gems, it is always free of trapiche motifs. One possible scenario for the development of trapiche tourmaline appears to be rapid crystal growth (i.e., somewhere between normal growth and skeletal growth; see also Sunagawa et al., 1999, and box A). The presence of this skeletal motif within the core formed by the $\{10\bar{1}1\}$ sector indicates that this trapiche tourmaline grew rapidly from the beginning of crystallization. Slightly faster growth at the edges would result in the formation of growth channels and the trapping of black inclusions to form the trapiche pattern. Evidence for rapid growth rates can be seen in snowflakes, which can show all stages from normal hexagonal growth to entirely dendritic growth (Libbrecht and Rasmussen, 2003). The channels were formed by rapid growth and the associated black inclusions were trapped in the tourmaline at the faster-growing edges, since a rapid growth rate is one factor that causes more inclusions to be trapped within a gem (Nassau and Jackson, 1970; Sumiya et al., 2005). The accumulation of black inclusions on the faces of the core formed by the $\{10\bar{1}1\}$ sector is likely related to a change in growth conditions.

CONCLUSION

These unusual green tourmalines from Zambia provide a rare example of tourmaline containing a skeletal trapiche pattern. The tourmaline samples analyzed are nearly pure uvite, colored by vanadium. The black pattern shown by slices of this trapiche tourmaline is formed by growth channels that contain carbonaceous material. The pattern is unusual in that there is a trigonal "star" in the core of the slices. The complex trapiche pattern is indicative of rapid growth of the tourmaline from the beginning of crystallization. Although tourmaline is relatively abundant at Kavungu, to date there has been very little organized mining and only a small percentage of the crystals recovered are suitable for slicing to show the trapiche pattern.

ABOUT THE AUTHORS

At the time this article was prepared, Mr. Hainschwang (thainschwang@yahoo.com) was research gemologist, and Mr. Notari was research manager, at GIA GemTechLab in Geneva, Switzerland. They are now research manager and laboratory manager, respectively, at GemTechLab in Geneva. Mr. Anckar worked for the European Union Mining Sector Diversification Programme in Lusaka, Zambia, and is currently a consulting geologist and gemologist residing in Göteborg, Sweden.

ACKNOWLEDGMENTS

The authors are grateful to Denis Gravier (Gravier & Gemmes, Poncin, France) for supplying samples; Andreas Ertl (Institut für Mineralogie und Kristallographie, Geozentrum–University of Vienna, Austria) for X-ray diffraction analysis and lattice parameter calculations; Dr. William B. Simmons and Alexander U. Falster (University of New Orleans, Louisiana) for electron-microprobe analysis; Dr. Andy H. Shen (GIA Laboratory, Carlsbad) for Raman analysis; and Elizabeth Quinn (GIA Laboratory, New York) for determination of standard gemological data. One of the authors (BA) gratefully acknowledges Stanley Kabwita, an amethyst miner and gem dealer from Solwezi, Zambia, for guiding him to the tourmaline locality, as well as Daniel Lombe and Emanuel Mulenga (both of the Geological Survey of Zambia, Lusaka) for fruitful comments on the mining area.

REFERENCES

Anovitz L.M., Grew E.S. (1996) Mineralogy, petrology and geochemistry of boron: An introduction. In E.S. Grew and L.M. Anovitz, Eds., *Boron—Mineralogy, Petrology and Geochemistry*, Reviews in Mineralogy, Vol. 13, Mineralogical Society of America, Washington, DC, pp. 1–40.

Benesch F. (1990) *Der Turmalin: Eine Monographie*. Verlag Urachhaus, Stuttgart, Germany, 380 pp.

Bertrand E. (1879) Compte-rendu de la séance du 13 Février 1879 [Report of the meeting of February 13, 1879]. *Bulletin de la Société Minéralogique de France*, Vol. 2, p. 31.

Dietrich R.V. (1985) *The Tourmaline Group*. Van Nostrand Reinhold Co., NY, 300 pp.

Donovan J.J., Tingle T.N. (1996) An improved mean atomic number background correction for quantitative microanalysis. *Journal of Microscopy*, Vol. 2, No. 1, pp. 1–7.

Dunn P.J. (1977a) Uvite, a newly classified gem tourmaline. *Journal of Gemmology*, Vol. 15, No. 6, pp. 300–308.

Dunn P.J. (1977b) Chromium in dravite. *Mineralogical Magazine*, Vol. 41, pp. 408–410.

Garnier V., Ohnenstetter D., Giuliani G., Schwarz D. (2002) Rubis trapiches de Mong Hsu, Myanmar. *Revue de Gemmologie a.f.g.*, No. 144, pp. 5–11.

Gübelin E.J. (1939) Die Mineralien im Dolomit von Campolungo (Tessin) [The minerals in the dolomite of Campolungo (Tessin)]. *Schweizerische Mineralogische und Petrographische Mitteilungen*, Vol. 14, pp. 326–442.

Klinck B.A. (1977) The geology of the Kabompo Dome area—Explanation of Degree Sheet No. 1224 NE Quarter. *Report of the Geological Survey of Zambia*, No. 44, 27 pp. Appended to report: Geological Map of the Kabompo Dome Area (1992), Geological Survey Department, Lusaka, Zambia.

Libbrecht K., Rasmussen P. (2003) *The Snowflake: Winter's Secret Beauty*. Voyageur Press, Stillwater, MN, 115 pp.

Muñoz G.O. (1948) *Esmeralda de Colombia*. Bank of the Republic of Colombia, Bogotá, pp. 122–123.

Nassau K., Jackson K.A. (1970) Trapiche emeralds from Chivor and Muzo, Colombia. *American Mineralogist*, Vol. 55, No. 3–4, pp. 416–427.

Pogue J.E. (1917) The emerald deposits of Muzo, Colombia. *Transactions of the American Institute of Mining Engineers*, Vol. 55, pp. 42–45.

Rosenberg P.E., Foit F.F. (1979) Synthesis and characterization of alkali-free tourmaline. *American Mineralogist*, Vol. 64, No. 1–2, pp. 180–186.

Schmetzer K. (1978) Vanadium III als Farbträger bei natürlichen Silikaten und Oxiden—ein Beitrag zur Kristallchemie des Vanadiums [Vanadium III as color carriers in natural silicates and oxides—A contribution to the crystal chemistry of vanadium]. Ph.D. dissertation, University of Heidelberg, Germany, 277 pp.

Schmetzer K., Bank H. (1979) East African tourmalines and their nomenclature. *Journal of Gemmology*, Vol. 16, No. 5, pp. 310–311.

Schmetzer K., Hänni H.A., Bernhardt H.-J., Schwarz D. (1996) Trapiche rubies. *Gems & Gemology*, Vol. 32, No. 4, pp. 242–250.

Sumiya H., Toda N., Satoh S. (2005) Development of high-quality large-size synthetic diamond crystals. *SEI Technical Review*, No. 60, pp. 10–16.

Sunagawa I., Bernhardt H.J., Schmetzer K. (1999) Texture formation and element partitioning in trapiche ruby. *Journal of Crystal Growth*, Vol. 206, No. 4, pp. 322–330.

Sunagawa I. (2005) *Crystals—Growth, Morphology and Perfection*. Cambridge University Press, Cambridge, UK, 295 pp.

Takahashi Y., Sunagawa I. (1998) Tourmaline: Morphological and compositional variations during the growth history of uvite single crystals. *Journal of Gemmology*, Vol. 26, No. 4, pp. 226–236.

Win K.K. (2005) Trapiche of Myanmar. *Australian Gemmologist*, Vol. 22, pp. 269–270.